TECHNICAL REPORT

ISO/TR 18394

Second edition
2016-05-01

Surface chemical analysis — Auger electron spectroscopy — Derivation of chemical information

Analyse chimique des surfaces — Spectroscopie des électrons Auger — Déduction de l'information chimique

Reference number
ISO/TR 18394:2016(E)

International Organization for Standardization

COPYRIGHT PROTECTED DOCUMENT

ISO copyright office
Ch. de Blandonnet 8 • CP 401
CH-1214 Vernier, Geneva, Switzerland
Tel. +41 22 749 01 11
Fax +41 22 749 09 47
copyright@iso.org
www.iso.org

Contents

Page

Foreword

ISO (the International Organization for Standardization) is a worldwide federation of national standards bodies (ISO member bodies). The work of preparing International Standards is normally carried out through ISO technical committees. Each member body interested in a subject for which a technical committee has been established has the right to be represented on that committee. International organizations, governmental and non-governmental, in liaison with ISO, also take part in the work. ISO collaborates closely with the International Electrotechnical Commission (IEC) on all matters of electrotechnical standardization.

The procedures used to develop this document and those intended for its further maintenance are described in the ISO/IEC Directives, Part 1. In particular the different approval criteria needed for the different types of ISO documents should be noted. This document was drafted in accordance with the editorial rules of the ISO/IEC Directives, Part 2 (see www.iso.org/directives).

Attention is drawn to the possibility that some of the elements of this document may be the subject of patent rights. ISO shall not be held responsible for identifying any or all such patent rights. Details of any patent rights identified during the development of the document will be in the Introduction and/or on the ISO list of patent declarations received (see www.iso.org/patents).

Any trade name used in this document is information given for the convenience of users and does not constitute an endorsement.

For an explanation on the meaning of ISO specific terms and expressions related to conformity assessment, as well as information about ISO's adherence to the WTO principles in the Technical Barriers to Trade (TBT), see the following URL: Foreword — Supplementary information.

The committee responsible for this document is ISO/TC 201, *Surface chemical analysis*, Subcommittee SC 7, *Electron spectroscopies*.

This second edition cancels and replaces the first edition (ISO/TR 18394:2006), which has been technically revised.

Introduction

This Technical Report provides guidelines for the identification of chemical effects on X-ray or electron-excited Auger-electron spectra and for using these effects in chemical characterization.

Auger-electron spectra contain information on surface/interface elemental composition as well as on the environment local to the atom with the initial core hole[1][2][3][4][5]. Changes in Auger-electron spectra due to alterations of the atomic environment are called chemical (or solid-state) effects. Recognition of chemical effects is very important in proper quantitative applications of Auger-electron spectroscopy and can be very helpful in identification of surface chemical species and of the chemical state of constituent atoms in surface or interface layers.

Surface chemical analysis — Auger electron spectroscopy — Derivation of chemical information

1 Scope

This Technical Report provides guidelines for identifying chemical effects in X-ray or electron-excited Auger-electron spectra and for using these effects in chemical characterization.

2 Normative references

The following documents, in whole or in part, are normatively referenced in this document and are indispensable for its application. For dated references, only the edition cited applies. For undated references, the latest edition of the referenced document (including any amendments) applies.

ISO 18115 (all parts), *Surface chemical analysis — Vocabulary*

3 Terms and definitions

For the purposes of this document, the terms and definitions given in ISO 18115 (all parts) apply.

4 Abbreviated terms

CCC	core-core-core (Auger-electron transition)
CCV	core-core-valence (Auger-electron transition)
CK	Coster-Kronig
c-BN	cubic boron nitride
CVV	core-valence-valence (Auger-electron transition)
DEAR-APECS	Dichroic Effect in Angle Resolved Auger-Photoelectron Coincidence Spectroscopy
h-BN	hexagonal boron nitride
IAE	Interatomic Auger Emission
ICD	Interatomic Coulomb Decay
PAES	Positron-Annihilation-induced Auger Electron Spectroscopy
REELS	Reflection Electron Energy-Loss Spectroscopy

5 Types of chemical and solid-state effects in Auger-electron spectra

Many types of chemical or solid-state effects can be observed in Auger-electron spectra[1][2][3][4][5]. Changes in the atomic environment of an atom ionized in its inner shell can result in a shift of the kinetic energy of the emitted Auger electron. In the case of X-ray-excited Auger-electron spectra, energy shifts of Auger parameters (i.e. kinetic-energy differences between Auger-electron peaks and the photoelectron peaks corresponding to the core levels involved in the Auger-electron process) can be detected as well. Furthermore, the line shape, the relative intensity and the satellite structure (induced by the intrinsic

excitation processes) of the Auger-electron lines can be considerably influenced by chemical effects, as can the structure of the energy-loss region (induced by extrinsic, electron-scattering processes) accompanying the intrinsic peaks. Strong chemical effects on the Auger-electron spectral shapes offer ways of identification of chemical species using the "fingerprint" approach.

In the case of electron-excited Auger-electron spectra, the Auger peaks are generally weak features superimposed on an intense background caused to a large extent by the primary electrons scattered inelastically within the solid sample. As a consequence, the differential Auger-electron spectrum is often recorded (or calculated from the measured spectrum) rather than the direct energy spectrum, facilitating the observation and identification of the Auger-electron peaks and the measurement of the respective Auger transition energies. Differentiation can, however, enhance the visibility of random fluctuations in recorded intensities, as shown in Figure 1. If chemical-state information is needed from a direct energy spectrum, then the relative energy resolution of the electron spectrometer should be better than 0,15 % (e.g. 0,05 % or 0,02 %). A poorer energy resolution causes a significant broadening of the Auger-electron peaks and prevents observation of small changes of spectral line shapes or peak energies as chemical-state effects in the spectra. A great advantage of electron-excited Auger-electron spectroscopy over X-ray excitation with laboratory X-ray source, however, is the possibility of using high lateral resolution and obtaining chemical-state maps of surface nanostructures.

NOTE 1 Auger-electron spectra can be reported with the energy scale referenced either to the Fermi level or to the vacuum level. Kinetic energies with the latter reference are typically 4,5 eV less than those referenced to the Fermi level, but the difference in energies for these two references can vary from 4,0 eV to 5,0 eV since the position of the vacuum level depends on the condition of the spectrometer and may, in practice, vary with respect to the Fermi level. When energy shifts are determined from spectra recorded on different instruments, use of different energy references should be taken into account.

NOTE 2 While the visibility of noise features in a differential spectrum can be reduced by use of a larger number of channels in the calculation of the derivative, there may also be distortion of the resulting differential spectrum and loss of fine details associated with chemical-state effects.

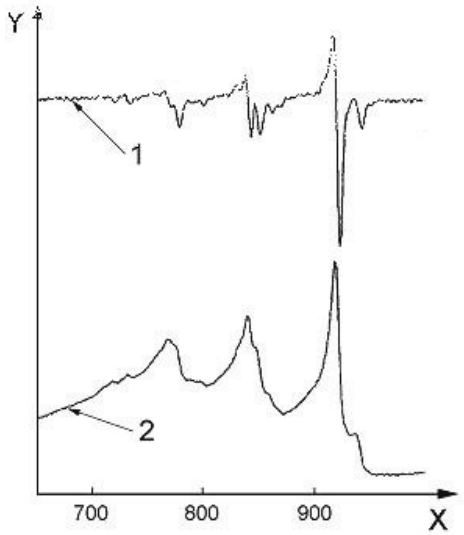

Key

X kinetic energy, eV
Y intensity
1 differential spectrum
2 direct spectrum

NOTE This figure is reproduced from Figure 2.8 of Reference [1].

Figure 1 — Comparison of direct and differentiated Auger-electron spectra for copper (Cu LMM peaks)

6 Chemical effects arising from core-level Auger-electron transitions

6.1 General

Core-level (or core-core-core, CCC) Auger-electron transitions occur when all of the levels involved in the Auger transition belong to the atomic core for the atom of interest.

6.2 Chemical shifts of Auger-electron energies

The main effect of any change in the solid-state environment on Auger-electron spectra for Auger transitions involving core levels is a shift of the Auger energies. This shift results from a change in the core atomic potential due to the changed environment and from a contribution due to the response of the local electronic structure to the appearance of core holes. Auger chemical shifts are generally larger than the binding-energy shifts of the atomic levels involved in the Auger-electron process because the two-hole final state of the process is more strongly influenced by relaxation effects. This phenomenon is illustrated by the example of aluminium and its oxide in Figure 2[6]. Large chemical shifts in the energy positions of the Auger-electron lines provide possibilities for chemical-state identification even in the case of electron-excited Auger-electron spectroscopy with, in this case, moderate energy resolution. In X-ray-excited Auger-electron spectra, the peak-to-background intensity ratios are usually larger than those in electron-excited spectra, facilitating accurate determination of peak energies. Recommended Auger electron energies are available for 42 elemental solids[7]. Information on Auger chemical shifts of particular elements can be obtained from handbooks[8][9][10][11] and online-accessible databases[12][13].

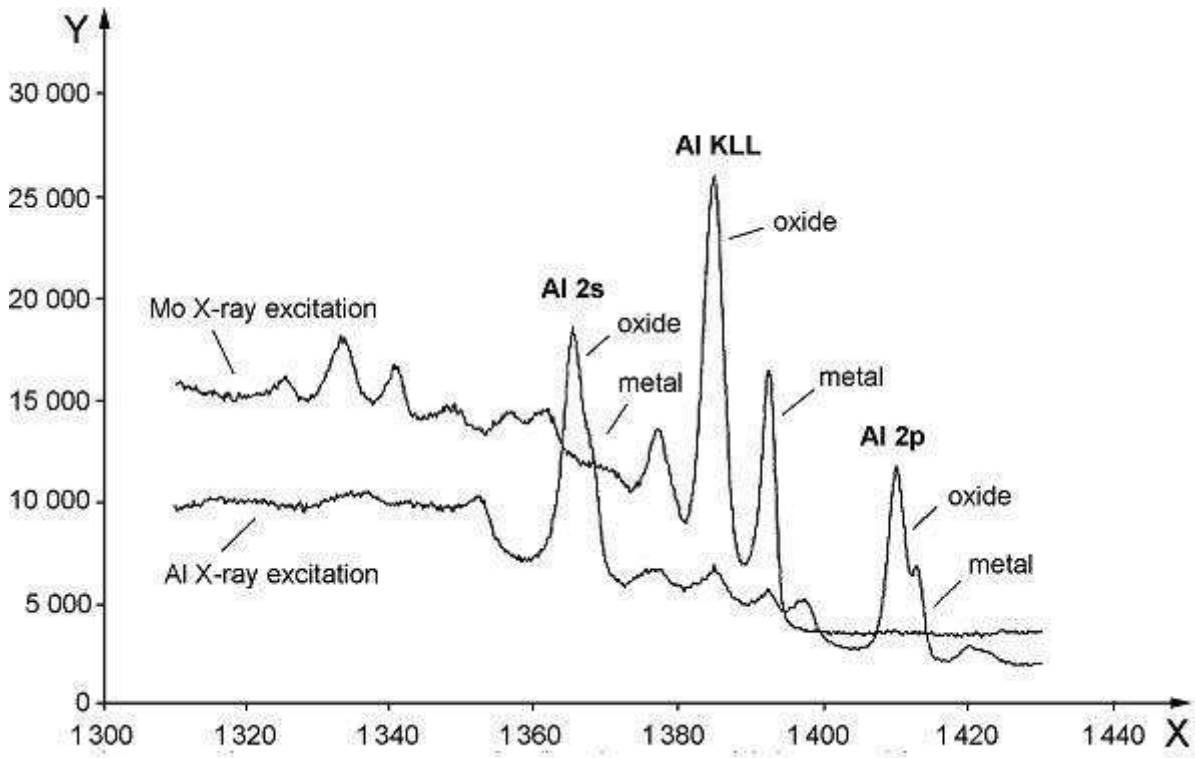

Key

X kinetic energy, eV

Y intensity, counts/s

Figure 2 — Photoelectron and Auger-electron spectra of an aluminium foil covered by a thin overlayer of aluminium oxide: Excitation with Al and Mo X-rays

With the advantage of high-energy-resolution analysers, small chemical shifts of Auger-electron lines due to different type of dopants in semiconductors become discernible (for example, the kinetic-energy difference between Si KLL peaks from *n*-type and *p*-type silicon is 0,6 eV[1]), allowing chemical-state mapping in spite of the extremely low concentration (far below the detection limits of Auger electron spectroscopy) of the dopants. Figure 3 shows a Si KLL Auger-electron map derived from a cross section of a *p*-type silicon sample doped with phosphorus by implantation to obtain *n*-type Si at the sample surface[1].

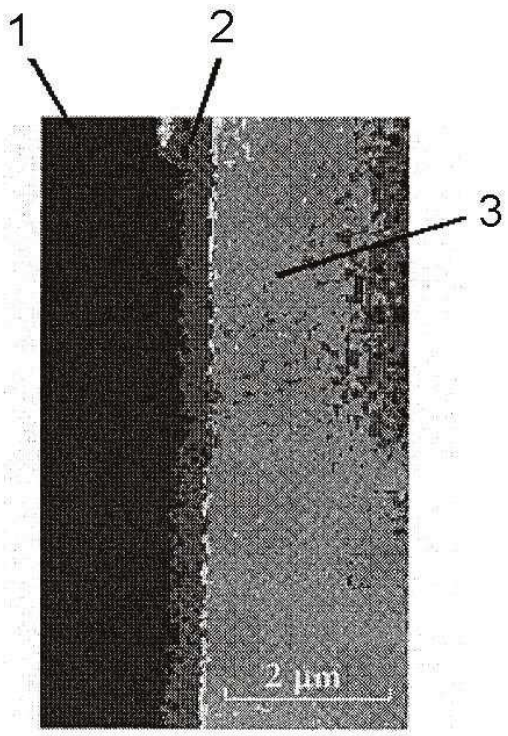

Key

1 vacuum

2 *n*-type Si (implanted with P)

3 *p*-type Si wafer

NOTE 1 A cross section of the sample is shown, and the Auger-electron spectra were excited with an electron beam.

NOTE 2 This figure has been reproduced from Figure 5.30 of Reference [1].

Figure 3 — Silicon KLL Auger-electron map of a *p*-type silicon sample implanted with phosphorus to produce *n*-type Si at its surface

6.3 Chemical shifts of Auger parameters

Auger parameters, obtained from X-ray-excited Auger-electron spectra, can also be strongly influenced by the environment of the atom emitting photoelectrons and Auger electrons[2][14][15][16][17][18]. The Auger parameter, α, is given by Formula (1):

$$\alpha = KE(jkl) - KE(i) \quad (1)$$

where

$KE(jkl)$ is the kinetic energy of an Auger transition involving core levels *j*, *k and l* of an atom;

$KE(i)$ is the kinetic energy of a photoelectron from core level *i* (which may be the same as the core level *j*).

In order to avoid negative values of the Auger parameter[14][15][16], the modified Auger parameter, α', is used in most practical cases. The modified Auger parameter is given by Formula (2):

$$\alpha' = \alpha + E_p = KE(jkl) + BE(i) \quad (2)$$

where

E_p is the exciting photon energy;

$BE(i)$ is the binding energy of an electron in the core level *i*.

It is also preferable to use α' rather than α because the value of α' is independent of E_p.

The Auger parameters can be measured even in the case of static charging, since any charging shift is cancelled as energy separations of peaks are determined. No energy-referencing problems occur[14][15] in the case of measuring Auger parameters; i.e. data obtained using the vacuum level as reference can be compared directly to data obtained using the Fermi level as reference. Auger parameters can therefore be very useful in the characterization of insulators and semiconductors, where the energy position of the Fermi level of the sample is not well defined. A change in the atomic environment of a core-ionized atom can result in a chemical shift of the corresponding Auger parameter. Auger-parameter shifts depend on differences in the valence charge in the initial ground state and in the final state (intra-atomic contribution), as well as on differences in the contribution to the relaxation process of all other atoms in the system (extra-atomic contribution)[16].

When the intra-atomic contribution is dominant, a local screening mechanism of the core hole takes place, while in the case when the extra-atomic contribution is dominant, the screening mechanism is assumed to be non-local. In the latter case, simple electrostatic models can be used for estimating the electronic polarization energy[5][16][17][18][19][20]. The model of Moretti[16] describes the final-state polarization process in which the sum of the electric fields (at the ligands) is generated by the central positive charge and by induced dipoles on the ligands in the first coordination shell. This model can be applied to estimate the extra-atomic polarization energy and the Auger-parameter shifts. Calculation of Auger parameter shifts using the electrostatic model of Moretti is facilitated by the possibility of applying the freely available Tinker molecular modelling and Molden computer graphic software packages[18]. Weightman, et al.[21][22] developed a different model, the “extended potential model”, for estimating the Auger-parameter chemical shift; potential parameters were derived from atomic calculations and the angular-momentum character of the electrons was taken into account. This model gives a good approximation in the case of large charge transfer in the final state (conductors), where the electrostatic model is not applicable, and describes well the local screening mechanism. In the case of binary alloys, the magnitude of the transferred charge can be accurately derived[3]. A review on first principles calculations of Auger kinetic energy and Auger parameter shifts in metallic bulk solids from the density functional theory are discussed in Reference[23].

In the case of nanoparticles, the Auger parameter can depend on the size of the particles. Figure 4 shows the dependence of the Auger parameter of Cu nanoclusters [deposited by evaporation onto highly oriented pyrolitic graphite (HOPG)] on the nominal thickness of the Cu layer[24]. It was found that the Cu Auger parameter depends linearly on $1/d$, where d is the average diameter of the Cu clusters[24].

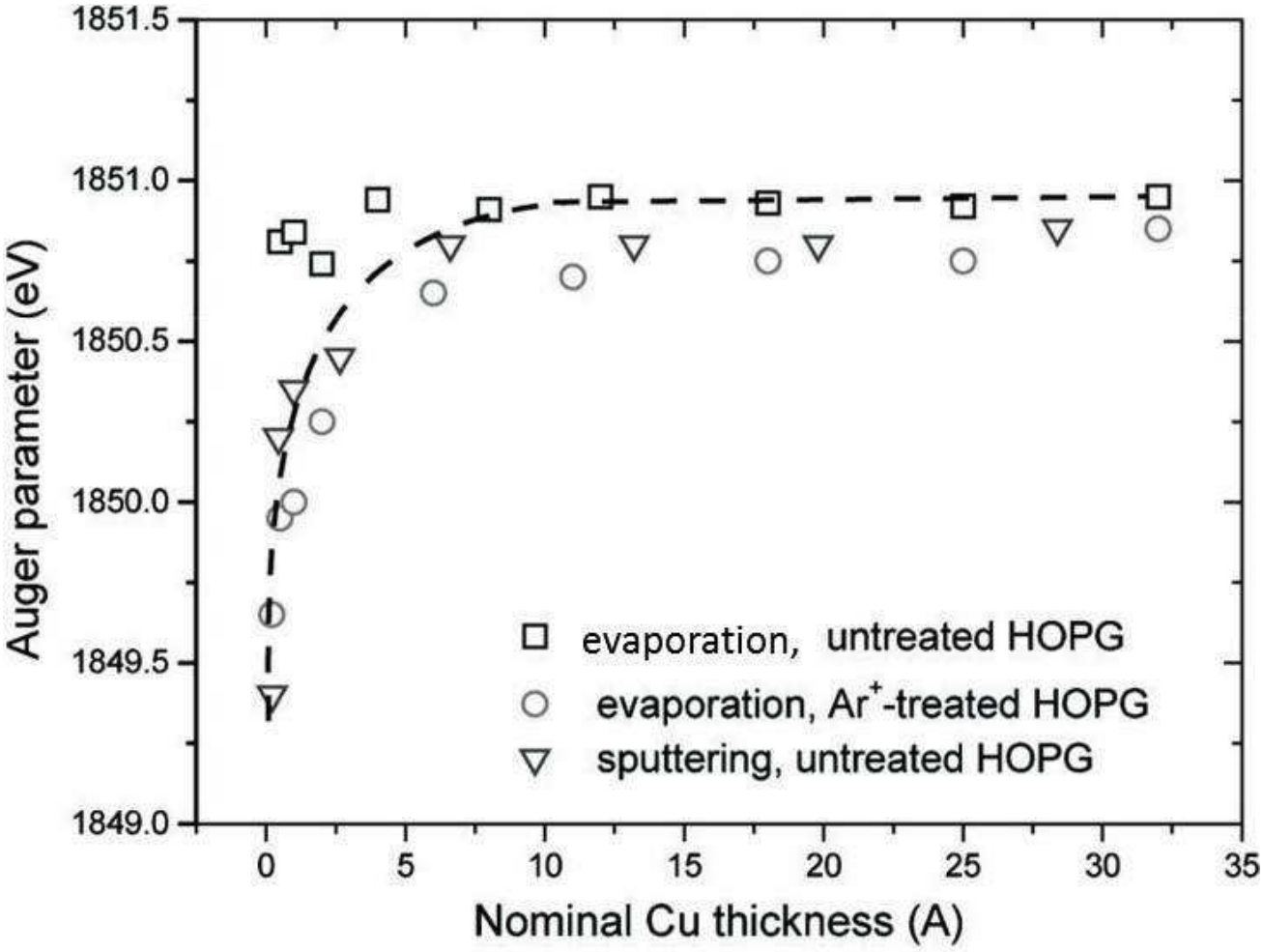

NOTE See Figure 2 of Reference[24].

Figure 4 — Dependence of the Cu Auger parameter on the nominal thickness of the Cu layer consisting of Cu clusters deposited by evaporation onto HOPG surface

6.4 Chemical-state plots

For chemical-state identification and Auger-parameter analysis, the presentation of Auger parameters in the form of a two-dimensional plot, as proposed by Wagner, proved to be very useful[15]. The Auger-electron kinetic energy is indicated on the ordinate of the plot and the corresponding photoelectron binding energy is on the abscissa but oriented in the negative direction, as shown in Figure 5; constant Auger-parameter values are represented on the plot by a straight line with a slope of –1 (note that the abscissa axis in Figure 5 is increasing to the left). In the case of a negligible change in the intra-atomic relaxation energy (due to the varying atomic environment), the change in the extra-atomic-relaxation (final-state-effect) energy dominates, and components with higher extra-atomic relaxation energy lie in the upper part of the chemical-state (or Wagner) plot. On the other hand, when the initial-state effects (proportional to the sum of terms related to the ground-state valence charge and the Madelung potential) dominate, the slope becomes –3 on the chemical-state plot; i.e. chemical states with similar initial-state effects lie on straight lines with a slope of –3. This result illustrates that chemical-state plots can be analysed to provide information on the nature of the changes in the environment of the core-ionized atom[19]. Figure 5 shows a chemical-state plot for tin compounds[25]. As can be seen, the chemical-state plot can help to distinguish between chemical states not separable on the basis of core-level binding energy shifts or Auger-electron-energy shifts alone.

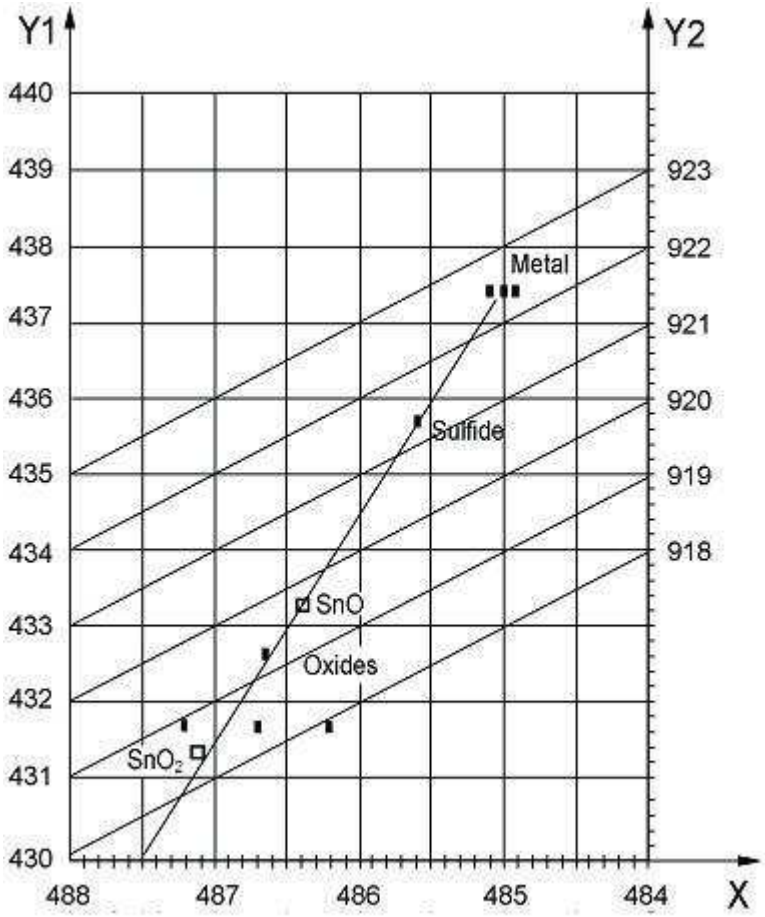

Key

X Sn $3d_{5/2}$ binding energy, eV

Y_1 Sn MNN Auger kinetic energy, eV

Y_2 Auger parameter + photon energy

NOTE Reprinted from Reference[25].

Figure 5 — Chemical-state plot for tin compounds

6.5 Databases of chemical shifts of Auger-electron energies and Auger parameters

The first comprehensive set of critically collected data on Auger parameters, Auger-electron kinetic energies and photoelectron binding energies for several elements is found in Reference.[15] A handbook contains a collection of experimental photoelectron binding-energy and Auger-electron kinetic-energy data for a large number of compounds[8] and includes several chemical-state plots. The latest version of the US National Institute of Science and Technology XPS Database[12] provides online access to over 33 000 records of photoelectron and Auger-electron data involving intense transitions for most elements and many compounds. This database supplies Auger parameters, has the option of displaying chemical-state plots, and is very useful for identification of chemical state as well as in studies of the dependence of polarization energy on chemical state. Auger-parameter values for 42 elemental solids are recommended in Reference[26].

6.6 Chemical effects on Auger-electron satellite structures

Auger-electron peaks can be accompanied by satellite lines due to intrinsic excitations. These excitations are often of atomic origin. As a consequence of the creation of the core hole, electrons can

be excited from occupied levels to unoccupied states (shake-up) or to the continuum (shake-off); the Auger-electron process then takes place in an excited or multiply ionized atom. Note that not only the shake-up but the shake-off process results in appearance of satellites in Auger-electron spectra, in contrast to photoelectron lines where the shake-off process induces a continuous energy contribution to the spectrum. The excited electron can be either a spectator or a participator in relation to the Auger transition. In this latter case, the energy of the Auger satellite can be even higher than that of the main line. Figure 6 shows an extraordinarily intense satellite occurring in the F KLL spectrum of polycrystalline KF; this satellite is interpreted as a resonance between the ground state and the core-ionized state[27]. Coupling of unpaired spins in the ionized core level and in the outer shell leads to multiple splitting of Auger lines; these splittings can be affected by changes in the atomic environment as well.

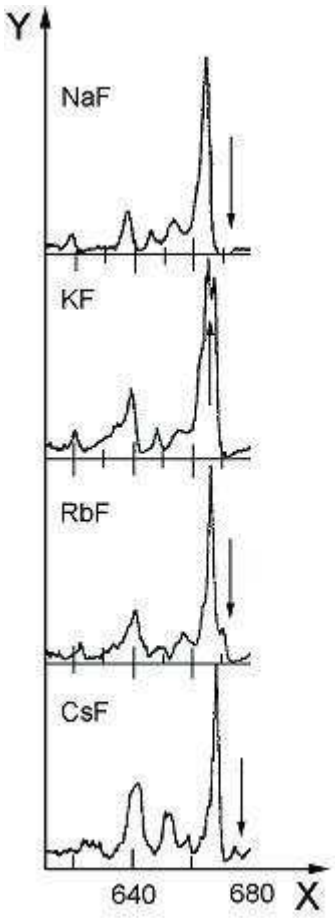

Key

X kinetic energy, eV

Y intensity

Figure 6 — Satellite structure (designated by arrows) in fluorine KLL Auger-electron spectra of fluorides

6.7 Chemical effects on the relative intensities and line shapes of CCC Auger-electron lines

The relative intensities of CCC Auger-electron transitions may change as a result of different Auger-transition probabilities in different atomic environments[28][29]. Very fast Coster-Kronig (CK) processes taking place prior to a particular Auger transition can convert the initial core hole into a vacancy in a core level with a smaller binding energy, leading to a considerable change in the relative intensities of

Auger transitions involving levels that participated in the CK process[30]. The probability of these CK processes can strongly depend on the chemical environment[31]. In the case of some metals, CCC Auger line shapes can be strongly asymmetric due to electron-hole pair excitation in the conduction band[32]. For adsorbates, a considerable broadening of the Auger-electron line can occur as a consequence of phonon excitation by the appearance of the core hole[33].

6.8 Chemical effects on the inelastic region of CCC Auger-electron spectra

Strong variations in the energy-loss structure of Auger-electron spectra can be observed, following changes of chemical state, e.g. in the case of some free-electron metals and their compounds. Figure 7 shows the difference between the KLL Auger spectra of metallic Al and Al_2O_3[34]. Reflection Electron Energy Loss Spectroscopy (REELS) can be used to confirm and separate chemical-state-dependent energy-loss structures in Auger-electron spectra. On the other hand, the interpretation of REELS spectra of multi-component systems can be confirmed by the surface chemical composition, obtained from quantitative Auger analysis[35].

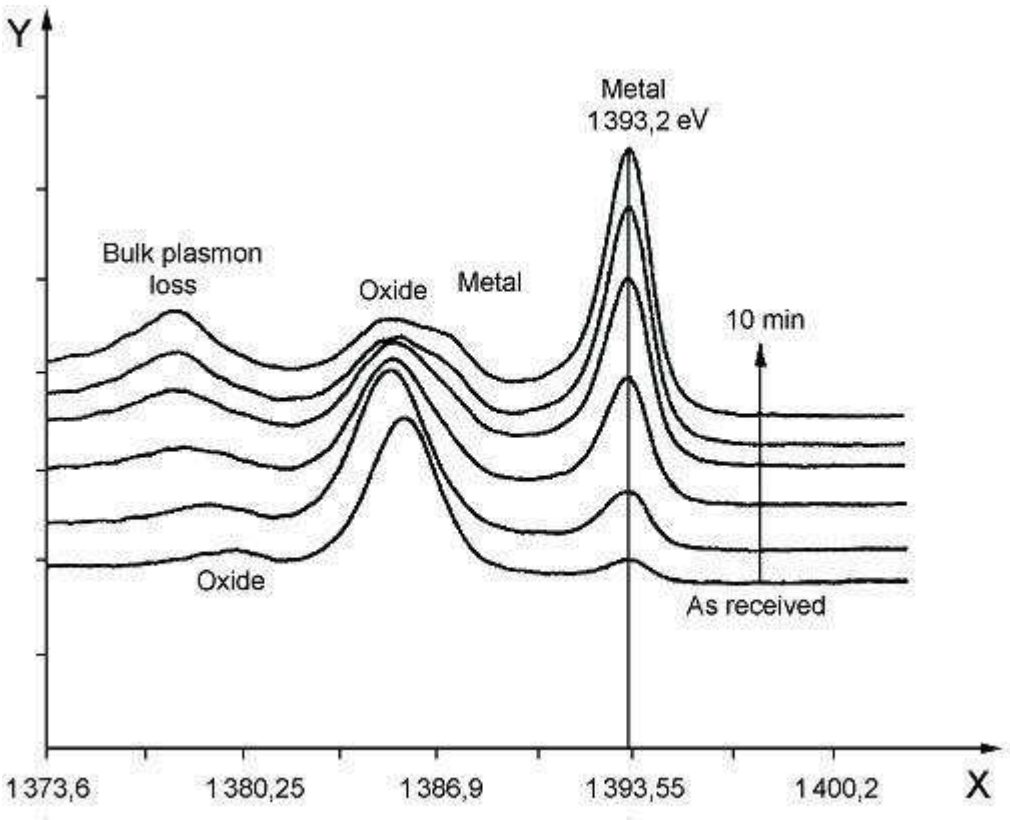

Key

X kinetic energy, eV

Y intensity

NOTE Reproduced from Figure 5 of Reference[34].

Figure 7 — Aluminium KLL Auger-electron spectra obtained by photo-excitation with Zr X-rays from an oxidized sample (lower curve) and after various times of ion sputtering to remove the oxide (upper curves)

7 Chemical effects on Auger-electron transitions involving valence electrons

7.1 General

In the case of Auger transitions involving valence electrons, the Auger-electron line shapes are expected to change due to changes in chemical state. The detection of these line shape changes may require high (better than 0,5 %) relative energy resolution, although the changes are observable at moderate energy resolution in many cases.

7.2 Chemical-state-dependent line shapes of CCV and CVV Auger-electron spectra

The line shapes of core-core-valence (CCV) and core-valence-valence (CVV) Auger-electron spectra can depend strongly on the environment (i.e. the chemical state) of the atoms emitting the Auger electrons. This effect can be utilized for fingerprinting, i.e. for identification of chemical state. Early measurements of carbon CVV Auger-electron spectra showed obvious differences in line shapes for graphite, diamond, metal carbides and carbon monoxide adsorbed on a metal surface[36][37]. Figure 8 shows electron-excited Si $L_{23}VV$ Auger-electron spectra of solid silicon and of various silicon compounds that show considerable differences in line shapes[38][39]. Figure 9 shows Pd $M_{45}N_{45}N_{45}$ Auger-electron spectra for different Cu-Pd and Ag-Pd alloys[40].

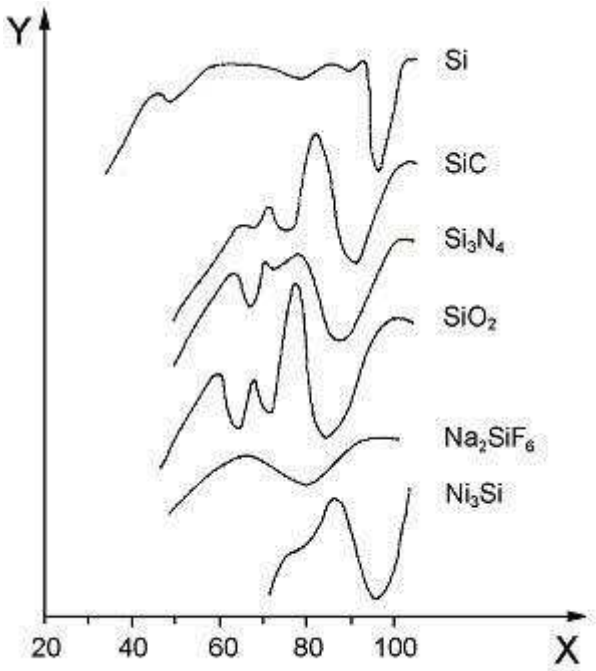

Key

X kinetic energy, eV

Y intensity

NOTE Reproduced from Reference[39].

Figure 8 — Silicon $L_{23}VV$ Auger-electron spectra in the differential mode for solid silicon and various silicon compounds

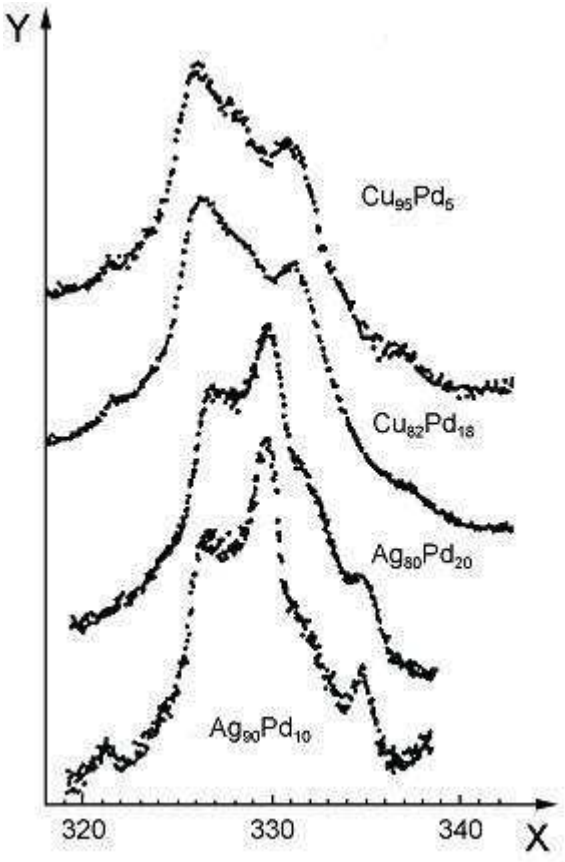

Key

X kinetic energy, eV

Y intensity

NOTE 1 Auger spectra were obtained with excitation by Mg X-rays.

NOTE 2 Reproduced from Reference[40].

Figure 9 — Palladium $M_{45}N_{45}N_{45}$ Auger-electron spectra for the indicated Cu-Pd and Ag-Pd alloys

The stronger effect of the environment on the CVV peak compared with the CCV or CCC peaks is shown clearly in the spectra of the metals and their oxides in the series Ti to Zn[41]. These spectra show how the environmental effect depends on the valence-level occupancy; this effect is a maximum in the middle of the Ti-Zn series.

Direct-mode, high-energy-resolution, electron-excited Ti $L_3M_{23}M_{45}$ Auger-electron spectra for TiN samples with relative N concentrations varying from 0 to 1,06 are shown in Figure 10[42]. The secondary peak on the low-kinetic-energy side of the main peak appears to be due to hybridization of the N 2p and Ti 3d states. The height of this peak relative to that of the main peak shows a linear dependence on the N/Ti concentration ratio; this relationship provides a simple method for determining the latter[42].

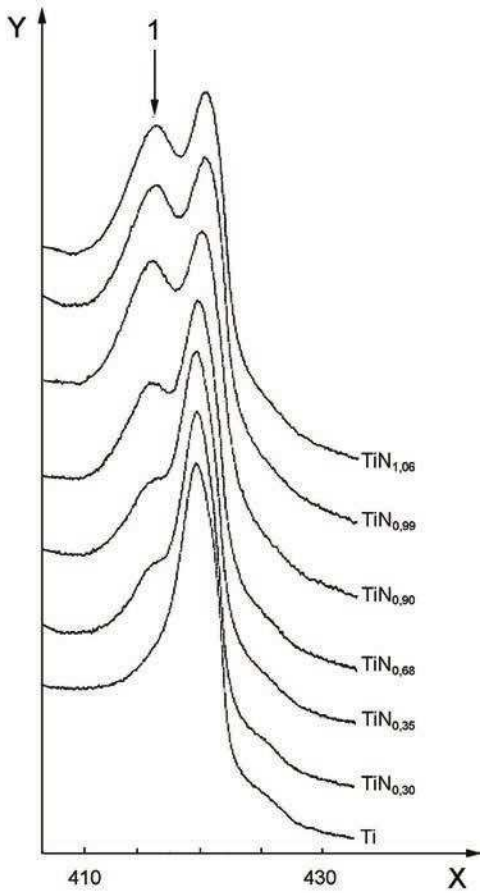

Key

X kinetic energy, eV

Y intensity

1 hybrid peak

NOTE 1 Auger spectra were obtained with electron excitation and an analyser of high energy resolution.

NOTE 2 Reproduced from Figure 2 of Reference[42].

Figure 10 — Titanium $L_3M_{23}M_{45}$ Auger-electron spectra of TiN samples of varying nitrogen concentrations

Boron KLL Auger-electron spectra of $TiB_{1,7}N_{1,8}$, TiB_2, cubic-BN (c-BN), and hexagonal-BN (h-BN) obtained in the differential mode are shown in Figure 11.[43] The agreement of the energies of the main peak (labelled by 1) in the spectra of $TiB_{1,7}N_{1,8}$ and of h-BN, as well as the similarity in the positions of the minor peaks in these spectra (labelled by 2 and 3) indicate that the BN in the $TiB_{1,7}N_{1,8}$ sample is present in the sp^2 hybridized hexagonal form[43].

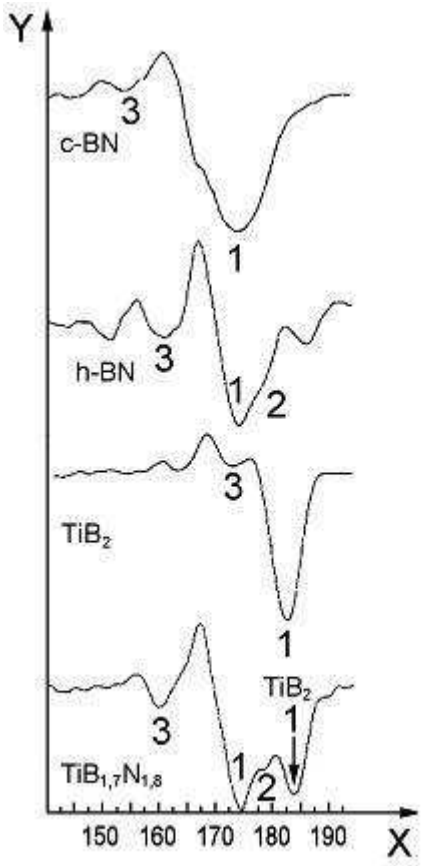

Key

X kinetic energy, eV

Y intensity

1 main peak

2 minor peak

NOTE Reprinted from Reference[43].

Figure 11 — Boron KLL Auger-electron spectra of $TiB_{1,7}N_{1,8}$, TiB_2, h-BN, and c-BN obtained in the differential mode

If a measured Auger-electron spectrum consists of components arising from different chemical species and the component spectra have different line shapes, factor analysis can be helpful in distinguishing the relevant spectral components. Least-squares fitting of the entire spectrum with varying contributions of component spectra is also helpful in interpreting the whole spectrum. These methods were successfully applied to quantitative studies of the oxidation of ternary alloys[44][45]. A comprehensive review of cases where chemical effects on Auger line shapes were predicted or used for chemical-state identification can be found in Reference[46].

The percentage ratio of the sp^2 and sp^3 hybridization states in the case of carbon materials can be determined from the energy separation between the most positive and most negative excursions (the *D* parameter) of the first derivative X-ray excited C KLL Auger line (the shape of which is sampling the valence band)[47]. Figure 12 illustrates the *D* parameter for different carbon materials[47] and *D* parameters as a function of percentage content of sp^2 hybrid bonds in several carbon materials are shown in Figure 13[48]. *D* parameters were used, e.g. for determining the sp^2 bond content in polymers irradiated by low electron dose[49] and in oxidized and purified multiwall carbon nanotubes[50].

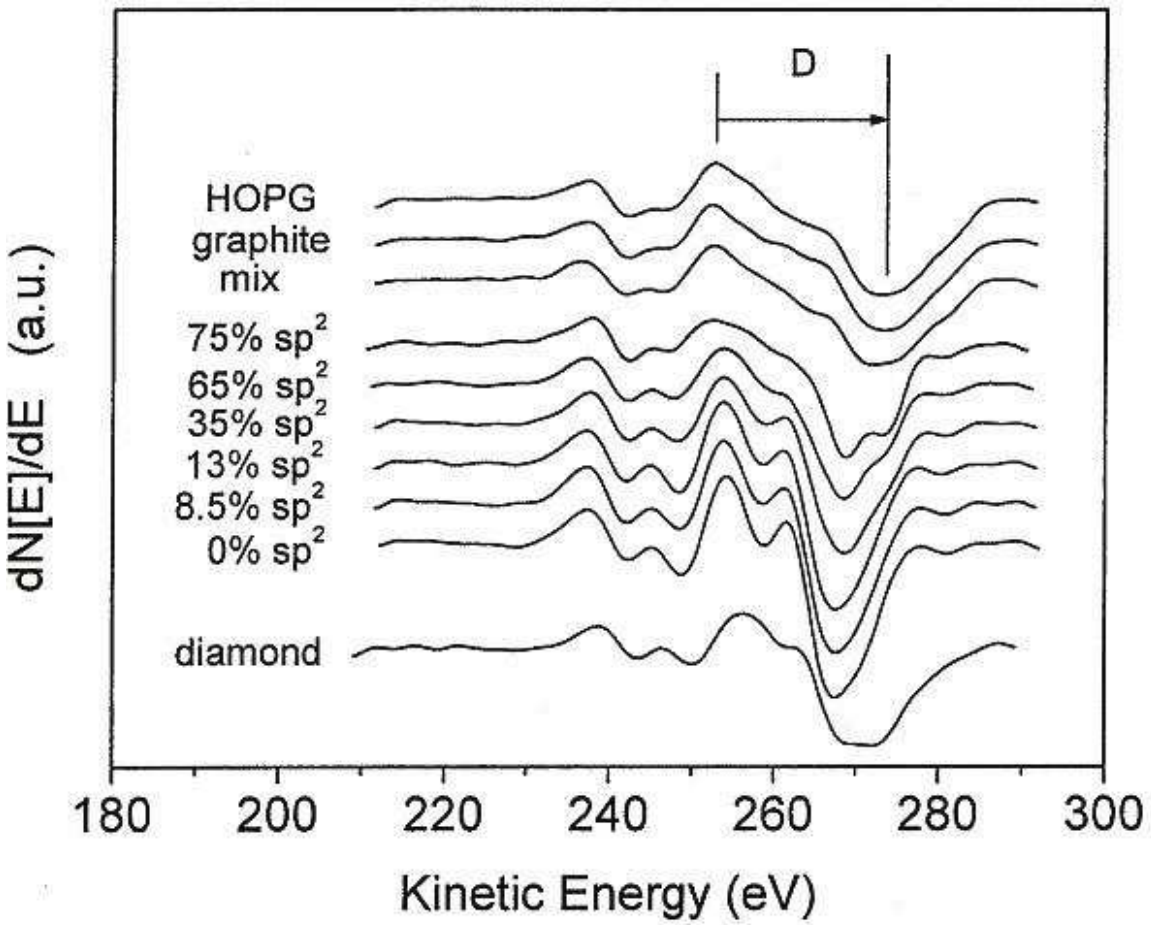

NOTE 1 The "mix" indicates a sample with a mixture of graphite powder and diamond powder.

NOTE 2 See Reference[47].

Figure 12 — First derivative C KLL spectra obtained from HOPG graphite, diamond and polystyrene-polyethylene copolymer samples

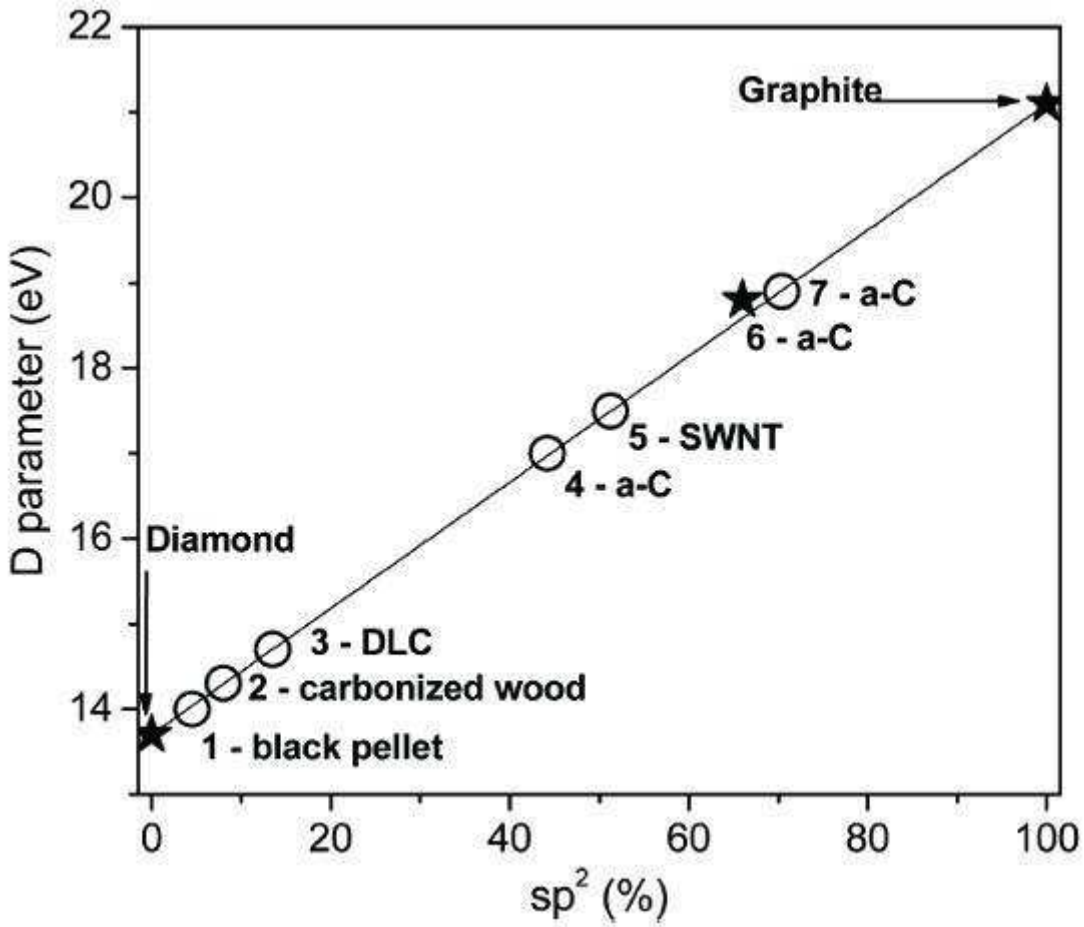

DLC diamond-like carbon

SWNT single-wall carbon nanotube

a-C amorphous carbon

NOTE See Reference[48].

Figure 13 — *D* parameters for some carbon materials vs percentage content of sp^2 hybrid bonds

7.3 Information on local electronic structure from analysis of CCV and CVV Auger-electron line shapes

Line shapes of CCV and CVV Auger-electron transitions can be analysed to give information on the local electronic structure of the emitting atom (i.e. on the local density of electronic states and on the magnitude of correlation effects)[3][4][51][54]. For the case of CCV Auger spectra of metals that have no contribution of *d* electrons in their conduction bands and for which the character of the initial state is very different from that of the final state, the "*final-state rule*" has been established for describing the spectral line shape[3]. According to this rule, the *line shape* is determined by the *partial (*sp*) local density of states in the final state*, and the *line intensities* are determined by the *local electronic configuration in the initial state.* For simple metals, this approach yields generally good agreement with experimental CCV and CVV line shapes[51]. The *final state rule* neglects electronic correlations between the two holes in the final state. In the case of *d* transition metals, however, the two final-state holes are in the *d* band and their interaction is usually strong, especially when the band is completely filled and the Coulombic repulsion between the holes is large compared to the bandwidth. In such cases, sharp, *quasi-atomic* line shapes are observed in CVV Auger-electron spectra[52][53][54]. The ratio of the Coulombic repulsion energy and the bandwidth can be varied by alloying, thus varying the strength of the quasi-atomic

component relative to that expected from the self-convolution of the valence-band density of states[3]. Interatomic Auger transitions where the core hole state in one atom is de-excited by electron emission from another atom and the corresponding interatomic Auger-electron spectra carry information on the local density of electronic states, e.g. in the case of adsorbate atoms on a transition-metal substrate[55]. Investigations of interatomic Auger transitions proved to be useful first in studying transition-metal oxides[56].

7.4 Novel techniques for obtaining information on chemical bonding from Auger processes

Positrons can also be used to induce Auger spectra from atoms at the uppermost layer of surfaces by annihilation with core level electrons[57]. This method is extremely surface sensitive and has been utilized in studies of effects of oxygen adsorption on properties of metal and semiconductor surfaces[58]. Figure 14 shows the Cu MVV positron-excited Auger-electron spectra (PAES) of a clean and previously oxidized Cu (100) surface following thermal anneals at 300 °C[58]. At the end of the annealing cycles the PAES spectrum looks similar to the PAES spectrum of the clean metal[58].

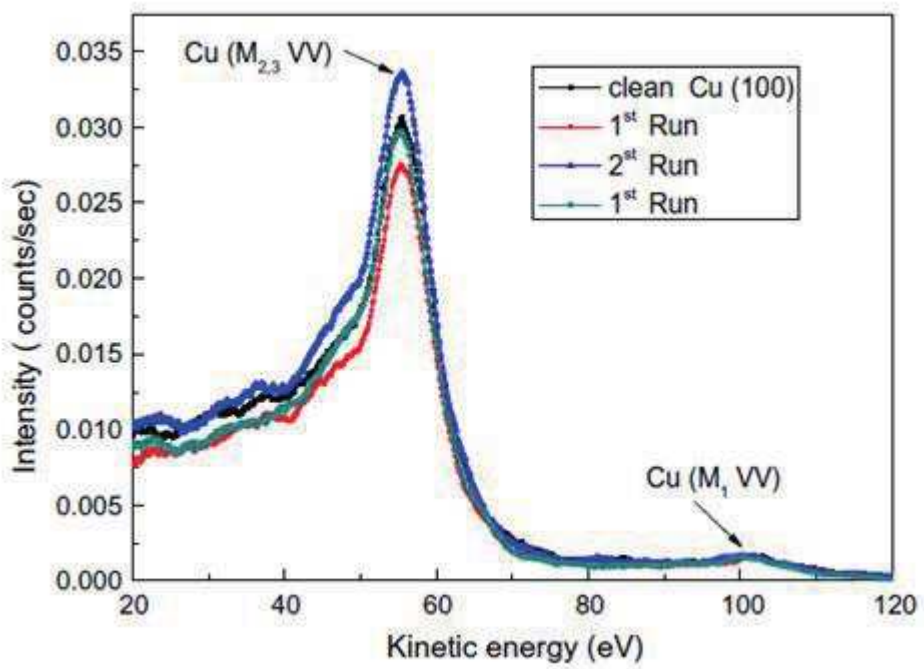

NOTE See Reference[58].

Figure 14 — Comparison of PAES spectra of a clean Cu (100) and a previously oxidized surface following annealing cycles at 300 °C

The dichroic effect in angle-resolved Auger-photoelectron coincidence spectroscopy (DEAR-APECS) was observed first by Gotter, et al.[59] The DEAR-APECS technique provides spin selectivity by selectively enhancing or suppressing the contributions from spin-symmetric (triplet) or spin-antisymmetric (singlet) Auger final-state configurations to the APECS spectra[59]. Figure 15 shows the experimental configurations of the DEAR-APECS[60]. In Figure 16 the APECS spectra of a CoO thin film, measured in two geometries are shown at temperatures lower and higher than the magnetic transition temperature[60]. The APECS spectra demonstrate the disappearance of the dichroism at high temperatures indicating the collapse of the short-range magnetic order[60].

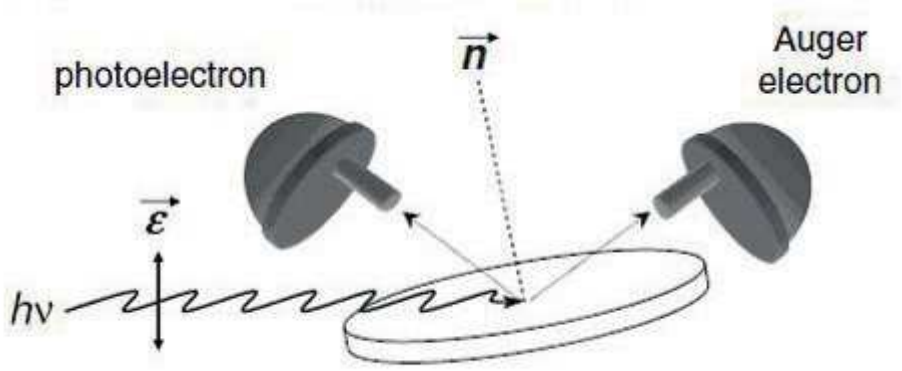

a) Configuration NN

Neither the direction of the detected photoelectrons, nor the direction of the Auger electrons are aligned with the direction of the polarization vector ε of the exciting photon beam (NN).

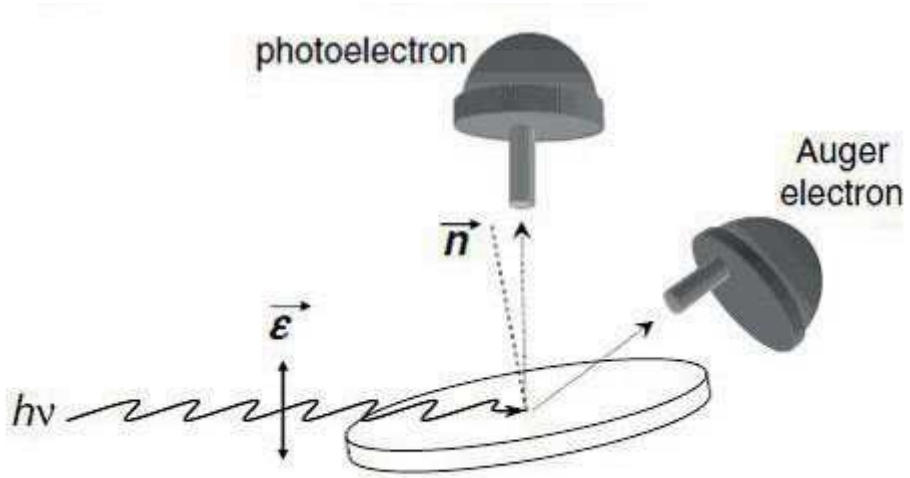

b) Configuration AN

The direction of photoelectrons is aligned with that of the photon polarization (A), while the direction of Auger electrons is not aligned (N).

NOTE See Reference[60].

Figure 15 — Two geometrical configurations for acquiring DEAR-APECS spectra

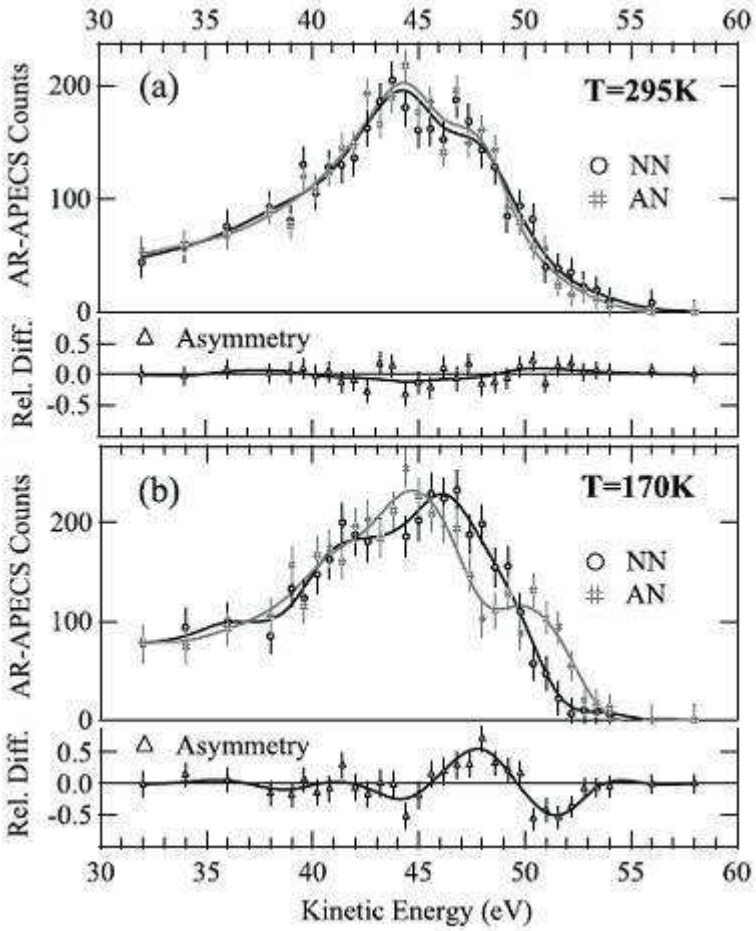

NOTE See Reference[60].

Figure 16 — Co $M_{23}VV$ Auger and Co 3p photoelectron coincidence spectra of CoO thin film measured in the NN and AN geometries, (a) above and (b) below the magnetic transition temperature

Following the core level photoionization, the core hole in a particular atom is generally filled by a subsequent Auger-decay process, e.g. by an inner-valence electron and the energy available is transferred to an outer-valence electron, the Auger electron that is emitted. In the case of molecules, clusters or solids, the hole left in the inner-valence level can decay rapidly through an Interatomic Coulomb Decay (ICD) process, illustrated in Figure 17[61]. The inner valence hole is filled by an outer valence electron of the same atom and the energy available is transferred to an outer valence electron, the ICD electron that is emitted[61]. The existence of this process predicted earlier by theoretical calculations has been proved by experiments and information on the progress in this field can be found in recent reviews[62] [63]. The process can be ultrafast and dominant in clusters multiply excited using ultrashort X-ray or laser photon pulses[64]. Detailed theoretical calculations have been recently published concerning ICD processes in small ammonia clusters[65] where the ICD channel can be controlled by protonation[66] and in small biochemically relevant hydrogen-bonded systems[66] where damaging low energy ICD electrons and cationic radicals are produced at the site of the biosystem participating in the ICD process, making the ICD a primary source of genotoxic particles[66]. Figure 18[66] shows the steps of the ICD process in systems where the water molecule interacts with HCHO (left) and a fragment of the enzyme lysozyme. It should be emphasized that the ICD following atomic Auger decay is a very general process and very important for many physical, chemical and biological phenomena where inner-shell vacancies in clusters are present[61]. It is hoped that ICD can appear in the near future as an extremely sensitive and efficient spectroscopic tool[63].

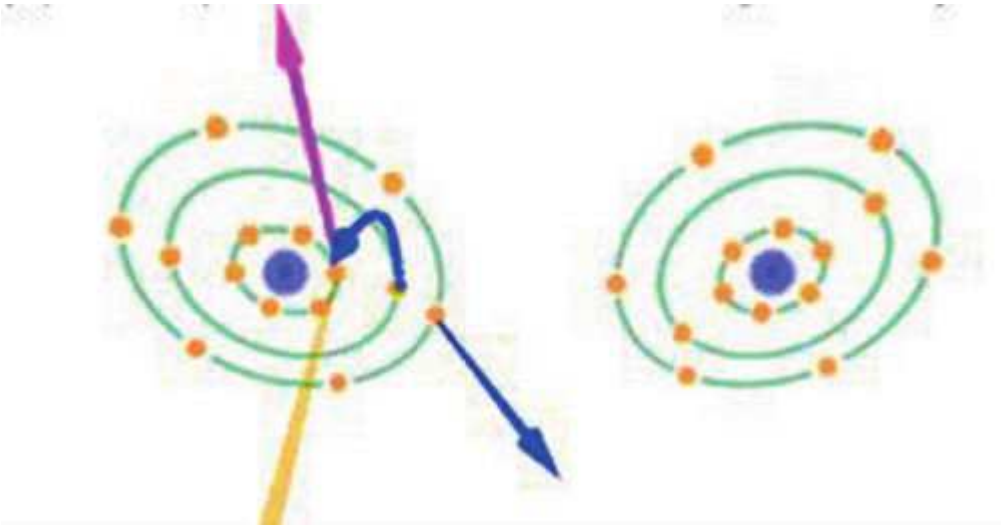

a) Core photoionization and Auger decay

Photoionization induces a 2p vacancy that is filled by a 3s electron and the Auger electron is emitted from the 3p level of the same atom.

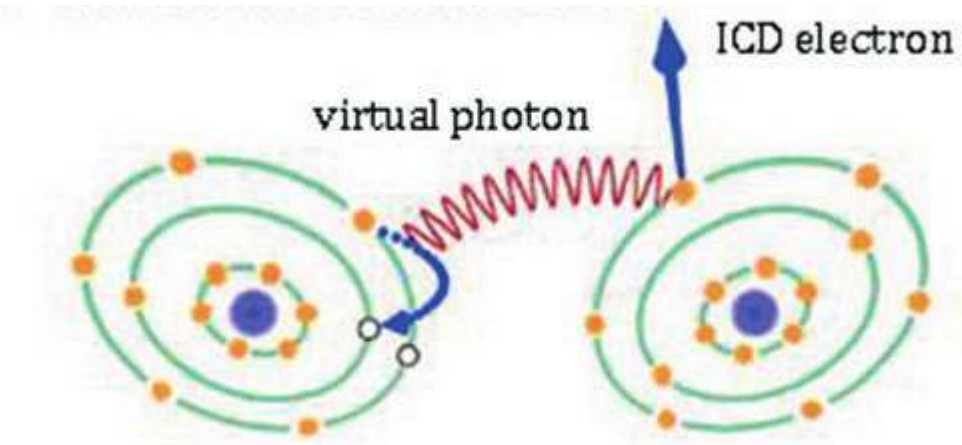

b) Interatomic Coulombic decay

In the subsequent ICD process, the 3s vacancy is filled by a 3p electron of the same atom and the excess energy is given to a 3p electron of the neighbouring atom.

c) Fragmentation

Fragmentation takes place due to Coulomb explosion.

NOTE See Reference[61].

Figure 17 — The ICD process in the Ar dimer

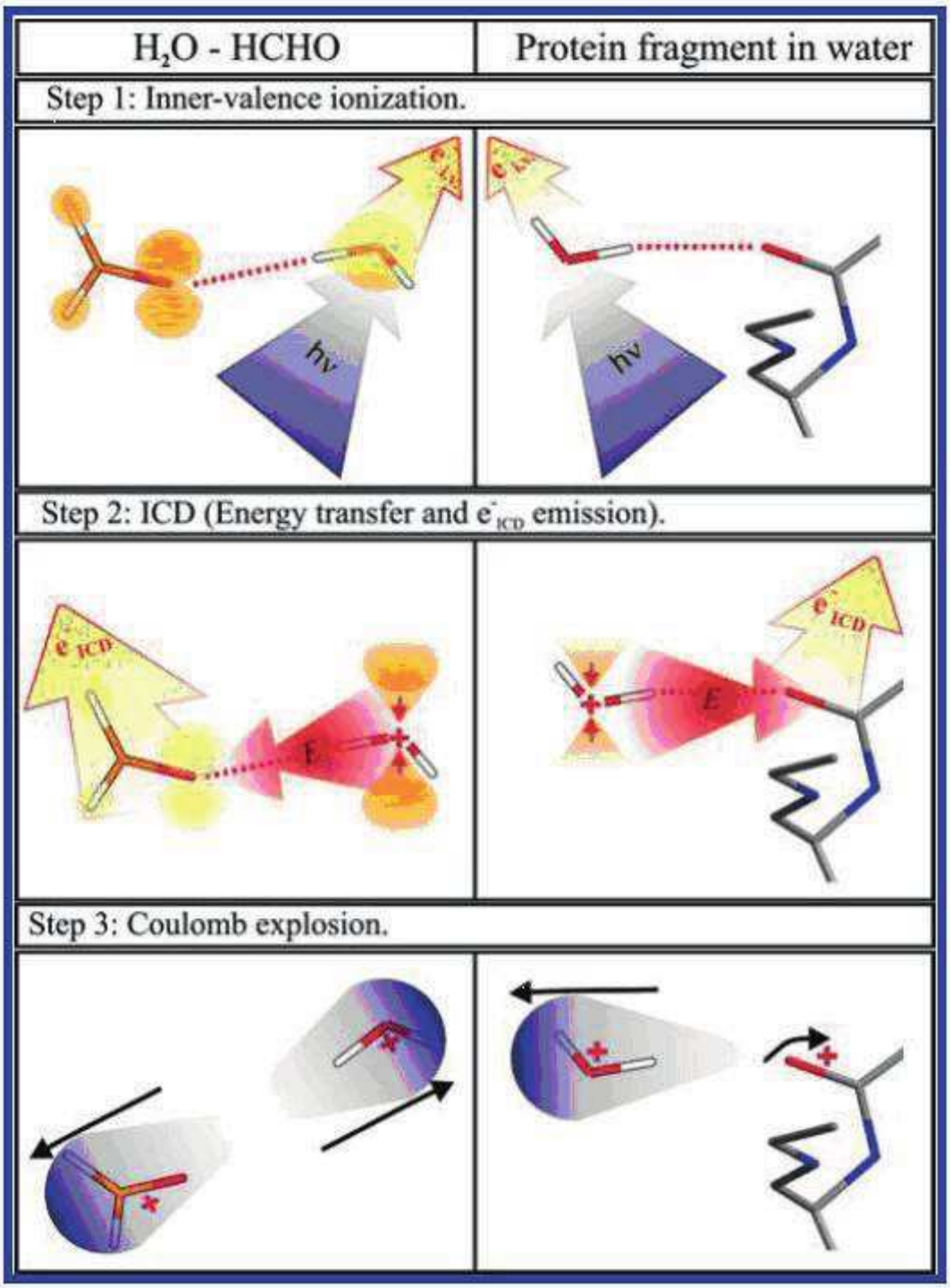

NOTE See Reference[66].

Figure 18 — Scheme of the ICD process in H_2O-HCH and in H_2O interacting with a fragment from the enzyme lysozyme

Bibliography

[1] WATTS J.F., & WOLSTENHOLME J. *An Introduction to Surface Analysis by XPS and AES*. John Wiley & Sons, Chichester, 2003

[2] MADDEN H.H. Chemical Information from Auger Electron Spectroscopy. *Journal of Vacuum Science and Technology.* 1981 April, **18** (3) pp. 677–689

[3] WEIGHTMAN P. Auger Spectroscopy and the Electronic Structure of Crystals. *Journal of Electron Spectroscopy and Related Phenomena.* 1994 May, **68** (1-4) pp. 127–138

[4] RAMAKER D.E. The Past, Present and Future of Auger Lineshape Analysis. *Critical Reviews in Solid State and Material Sciences.* 1991, **17** (3) pp. 211–276

[5] WAGNER C.D., & BILOEN P. X-ray Excited Auger and Photoelectron Spectra of Partially Oxidized Magnesium Surfaces: The Observation of Abnormal Chemical Shifts. *Surface Science.* 1973 March, **35** pp. 82–95

[6] TÓTH J., & KÖVÉR L. Files 00003266 and 00003267, *COMPRO, Common Data Processing System*, Version 8; available at http://www.sasj.gr.jp

[7] POWELL C.J. Recommended Auger-electron kinetic energies for 42 elemental solids. *Journal of Electron Spectroscopy and Related Phenomena.* 2010, **182** pp. 11–18

[8] MOULDER J.F., STICKLE W.F., SOBOL P.E., BOMBEN K.D. In: *Handbook of X-ray Photoelectron Spectroscopy*. (CHASTAIN J. ed.). Physical Electronics Inc., Eden Prairie, 1992

[9] *Handbook of X-ray Photoelectron Spectroscopy*IKEO N., IIJIMA Y., NIIMURA N., SIGEMATSU M., TAZAWA T., MATSUMOTO S., KOJIMA K., NAGASAWA Y. eds.), JEOL, Akishima, 1991

[10] CRIST B.V. *Handbooks of Monochromatic XPS Spectra, Three-Volume Set, no. 3.* John Wiley & Sons, 2000

[11] SURFACE ANALYSIS BY AUGER AND X-RAY PHOTOELECTRON SPECTROSCOPY. BRIGGS D., & GRANT J.T. eds.). IM Publications and SurfaceSpectra Limited, Chichester, 2003

[12] X-RAY PHOTOELECTRON SPECTROSCOPY DATABASE. Version 4.1, Standard Reference Database 20, National Institute of Standards and Technology, Gaithersburg, 2012. Accessible at: http://srdata.nist.gov/xps

[13] SURFACE ANALYSIS SOCIETY OF JAPAN. home page: http://www.sasj.gr.jp

[14] WAGNER C.D. Chemical Shifts of the Auger Lines and the Auger Parameter. *Faraday Discussions of the Chemical Society*. 1975, **60** pp. 291–300

[15] WAGNER C.D., & JOSHI A. The Auger parameter, its Utility and Advantages: A Review. *Journal of Electron Spectroscopy and Related Phenomena.* 1988 July, **47** (1) pp. 283–313

[16] MORETTI G. Auger Parameter and Wagner Plot in the Characterization of Chemical States by X-ray Photoelectron Spectroscopy: a Review. *Journal of Electron Spectroscopy and Related Phenomena.* 1998 August, **95** (2-3) pp. 95–144

[17] MORETTI G. The Auger Parameter. In: *Surface Analysis by Auger and X-Ray Photoelectron Spectroscopy*, (BRIGGS D., & GRANT J. eds.). IM Publications, Chichester, 2003, pp. 501–30.

[18] SATTA M., & MORETTI G. Auger parameters and Wagner plots, *Journal of Electron Spectroscopy and Related Phenomena.* (Special issue: Trends in X-ray Photoelectron Spectroscopy (theory, techniques and applications), guest ed. Kövér L.), 2010 May, **178-179**, pp. 123-127

[19] MATTHEW J.A.D. Core Hole Screening for Intermediate Size Metal Particles. *Solid State Communications.* 1990 January, **73** (2) pp. 179–183

[20] CITRIN P.H., & THOMAS T.D. X-ray Photoelectron Spectroscopy of Alkali Halides. *Journal or Chemical Physics.* 1972 November 15, **57** (10) pp. 4446–4461

[21] THOMAS T.D., & WEIGHTMAN P. Valence Electronic Structure of AuZn and AuMg Alloys Derived from a New Way of Analyzing Auger-Parameter Shifts. *Physical Review B.* 1986 April 15, **33** (8) pp. 5406–5413

[22] COLE R.J., MATTHEW J.A.D., WEIGHTMAN P. Extra-Atomic Relaxation Energy Calculations Using an Extended Potential Model. *Journal of Electron Spectroscopy and Related Phenomena.* 1995 March, **72** (3) pp. 255–259

[23] OLOVSSON W., MARTEN T., HOLMSTRÖM E., JOHANSSON B., ABRIKOSOV I. A Guest Ed. Kövér L. First principle calculations of core-level binding energy and Auger kinetic energy shift in metallic solids, *Journal of Electron Spectroscopy and Related Phenomena.* (Special issue: Trends in X-ray Photoelectron Spectroscopy (theory, techniques and applications), May 2010, **178-179**, pp. 88-99

[24] YANG D.Q., & SACHER E. Initial- and final-state effects on metal cluster/substrate interactions, as determined by XPS: copper clusters on Dow Cyclotone and highly oriented pyrolitic graphite. *Applied Surface Science.* 2002, **195** pp. 187–195

[25] KÖVÉR L., MORETTI G., KOVÁCS Zs., SANJINÉS R., CSERNY I., MARGARITONDO G. High Resolution Photoemission and Auger Parameter Studies of Electronic Structure of Tin Oxides. *Journal of Vacuum Science and Technology A*. 1995 May, **13** (3) pp. 1382–1388

[26] POWELL C.J. Recommended Auger parameters for 42 elemental solids. *Journal of Electron Spectroscopy and Related Phenomena.* 2012, **185** pp. 1–3

[27] UDA M., YAMAMOTO T., TAKENAGA T. Resonant Orbital Rearrangement During F 1s Ionization or Decay Process. *Advance Quantum Chemistry.* 1997, **29** pp. 389–419

[28] WEISSMANN R. Intensity Ratios of the KL_1 L_1 , KL_{23} L_{23} Oxygen Auger Lines in Different Compounds. *Solid State Communications.* 1979 August, **31** (5) pp. 347–349

[29] SARMA D.D., HEGDE M.S., RAO C.N.R. An Auger Spectroscopic Study of Surface Oxidation of Zinc. *Chemical Physics Letters.* 1980 August 1, **73** (3) pp. 443–446

[30] MÅRTENSSON N., & NYHOLM R. Electron Spectroscopic Determinations of *M* and *N* Core-Hole Lifetimes for the Elements Nb—Te (Z = 41-52). *Physical Review B*. 1981 December 15, **24** (12) pp. 7121–7134

[31] KÖVÉR L., CSERNY I., BRABEC V., FIŠER M., DRAGOUN O., NOVÁK J. 3*p* and 3*d* Core-Level Widths in Metallic Technetium: A Study by Internal-Conversion Electron Spectroscopy. *Physical Review B*. 1990 July 1, **42** (1) pp. 643–647

[32] DONIACH S., & SUNJIC M. Many-Electron Singularity in X-ray Photoemission and X-ray Line Spectra from Metals. *Journal of Physics C: Solid State Physics.* 1970 February, **3** (2) pp. 285–291

[33] MATTHEW J.A.D. Comparison of Vibrational Broadening in Auger and Photoelectron Spectroscopy. *Physical Review B*. 1984 March 15, **29** (6) pp. 3031–3034

[34] ALLGEYER D.F., & PRATZ E.H. XPS Analysis of Thin Oxide Films on Chemically Treated Aluminium Alloy Surfaces using a High–Energy Mg/Zr Anode. *Surface and Interface Analysis.* 1992 July, **18** (7) pp. 465–474

[35] STRYDOM I. le R., & HOFMANN S. XPS and EELS Study of the Valence Band Electronic Structure of TiN and (Ti, Al)N Coatings as Influenced by the Deposition Parameters. *Vacuum.* 1990, **41** (7-9) pp. 1619–1623

[36] Grant J.T., & Haas T.W. Auger Electron Spectroscopy Studies of Carbon Overlayers on Metal Surfaces. *Surface Science.* 1971 Jan., **24** (1) pp. 332–334

[37] Haas T.W., Grant J.T., Dooley G.J. Chemical Effects in Auger Electron Spectroscopy. *Journal of Applied Physics*. 1972 April, **43** (4) pp. 1853–1860

[38] Streubel P. Augerelektronspektroskopie (AES) zur Untersuchung von Festkörperoberflächen – Stand und Neuere Entwicklungen auf den Gebieten der Quantitativen Analyse und der Chemischen Information. *Zeitschrift für Chemie.* 1983 February, **23** (2) pp. 41–51

[39] Streubel P., Fellenberg R., Reif A. Interpretation of Auger Energy Shifts of Silicon in Solid Silicon Compounds. *Journal of Electron Spectroscopy and Related Phenomena.* 1984, **34** (3) pp. 261–274

[40] Weightman P., Andrews P.T., Winter H. Band Structure Effects on the Pd M_{45} N_{45} N_{45} Auger Spectra of Cu_x Pd_{1-x} and Ag_x Pd_{1-x} Alloys. *Journal of Physics C: Solid State Physics.* 1983 January, **16** (3) pp. L81–L87

[41] Seah M.P., Gilmore I.S., Bishop H.E., Lorang G. Quantitative AES, V. Practical analysis of intensities with detailed examples of metals and their oxides. *Surface and Interface Analysis.* 1998 September, **26** (10) pp. 701–722

[42] Haupt J., Baker M.A., Stroosnijder M.F., Gissler W. Auger Electron Spectroscopy Studies on TiN_x, *Surface and Interface Analysis,* July 1994, **22**, no. 1-12, pp. 167-170

[43] Baker M.A., Mollart T.P., Gibson P.N., Gissler W. Combined X-ray Photoelectron/Auger Electron Spectroscopy/Glancing Angle X-ray Diffraction/Extended X-ray Absorption Fine Structure Investigation of TiB_xN_y Coatings, *Journal of Vacuum Science and Technology*, March 1997, **15**, No. 2, pp. 284-291

[44] Hofmann S., & Steffen J. Factor Analysis and Superposition of Auger Electron Spectra Applied to Room Temperature Oxidation of Ni and $NiCr_{21}$ Fe_{12}. *Surface and Interface Analysis.* 1989 January-February, **14** (1-2) pp. 59–65

[45] Steffen H.J., , & Hofmann S. Quantitative Studies of the Initial Oxidation Stages of FeCrNi alloys using Factor Analysis and Least-squares Fitting Methods Applied to Low Energy AES spectra, *Surface and Interface Analysis*, June 1992, **19**, no. 1-12, pp. 157-160

[46] Ramaker D.E. Chemical Information from Auger Lineshapes. In: *Surface Analysis by Auger and X-Ray Photoelectron Spectroscopy*, (Briggs D., & Grant J. eds.). IM Publications, Chichester, 2003, pp. 465–500.

[47] TURGEON S., & PAYNTER R.W. On the determination of carbon sp^2/sp^3 ratios in polystyrene-polyethylene copolymers by photoelectron spectroscopy. *Thin Solid Films*. 2001, **394** pp. 44–48

[48] KACIULIS S. Spectroscopy of carbon: from diamond to nitride films. *Surface and Interface Analysis* 2012, **44** pp. 1155–1161

[49] LESIAK B., ZEMEK J., HOUDKOVA J. Hydrogen detection and quantification at polymer surfaces investigated by elastic peak electron spectroscopy (EPES). *Polymer.* 2008, **49** pp. 4127–4132

[50] STOBINSKI L., LESIAK B., KÖVÉR L., TÓTH J., BINIAK S., TRYKOWSKI G., JUDEK J. Multiwall carbon nanotubes purification and oxidation by nitric acid studied by the FTIR and electron spectroscopy methods. *Journal of Alloys and Compounds.* 2010, **501** pp. 77–84

[51] Fowles P.S., Inglesfield J.E., Weightman P. A First Principles Calculation of the KLV Auger Profiles of Simple Metals. *Journal of Physics: Condensed Matter.* 1991 February, **3** (6) pp. 641–653

[52] Cini M. Density of States of Two Interacting Holes in a Solid. *Solid State Communications.* 1976 November, **20** (6) pp. 605–607

[53] Cini M. Two Hole Resonances in the XVV Auger Spectra of Solids. *Solid State Communications.* 1977 December, **24** (9) pp. 681–684

[54] Sawatzky G.A. Quasiatomic Auger Spectra in Narrow-Band Materials. *Physical Review Letters.* 1977 August 22, **39** (8) pp. 504–507

[55] SALMERÓN M, BARÓ A.M.,, ROJO J.M., Interatomic transitions and relaxation effects in Auger spectra of several gas adsorbates on transition metals. *Physical Review B*. 1976 May 15, **13** pp. 4348–4363

[56] RAO C.N.R., & SARMA D.D. Interatomic Auger transitions in transition-metal oxides. *Physical Review B*. 1982 February 15, **25** pp. 2927–2929

[57] OHDAIRA T., & SUZUKI R. Positron-Annihilation-Induced Auger Electron Spectroscopy. In: *Surface Analysis by Auger and X-Ray Photoelectron Spectroscopy*. (Briggs D., & Grant J.T. eds.). IM Publications, Chichester, 2003, pp. 775–87.

[58] FAZLEEV N.G.,, NADESALINGAM M.P.,, MADDOX W.,, MUKHERJEE S.,, RAJESHWAR K.,, WEISS A. Oxidation and thermal reduction of the Cu(1 0 0) surface as studied using positron annihilation induced Auger electron spectroscopy (PAES). *Surface Science.* 2010, **604** pp. 32–37

[59] GOTTER R., DA PIÉVE F.,, RUOCCO A., OFFI F., STEFANI G., BARTYNSKI R. A., Dichroic effects in Auger photoelectron coincidence spectroscopy of solids. *Physical Review B*. 2005, **72** pp. 235409–1, 235409–5

[60] GOTTER R., OFFI F., RUOCCO A., DA PIÉVE F., STEFANI G., BARTYNSKI R. A.,, CINI M. Evidence for the collapse of short-range magnetic order in CoO at the Néel temperature, *Europhysics Letters,* May 2011, **94**, pp. 37008-1-37008-6

[61] MORISHITA Y., LIU X.J.,, SAITO N.,, LISCHKE T.,, KATO M.,, PRÜMPER G., OURA M.,, YAMAOKA H., TAMENORI Y., SUZUKI I. H.,, UEDA K. Experimental Evidence of Interatomic Coulombic Decay from the Auger Final States in Argon Dimers. *Physical Review Letters.* 2006, **96** pp. 243402–1, 243402–243404

[62] HERGENHAHN U. Interatomic and intermolecular coulombic decay: The early years. *Journal of Electron Spectroscopy and Related Phenomena.* 2011, **184** pp. 78–90

[63] AVERBUKH V., DEMEKHIN Ph. V., KOLORENČ P., SCHEIT S., STOYCHEV S. D., KULEFF A. I., CHIANG Y. C., GOKHBERG K., KOPELKE S., SISOURAT N., CEDERBAUM L. S. Interatomic electronic decay processes in singly and multiply ionized clusters. *Journal of Electron Spectroscopy and Related Phenomena.* 2011, **183** pp. 36–47

[64] KULEFF A. I., GOKHBERG K., KOPELKE S., CEDERBAUM L. S. Ultrafast Interatomic Electronic Decay in Multiply Excited Clusters, *Physical Review Letters,* 2010, 105, pp. 43004-1-43004-4

[65] KRYZHEVOI N., , & CEDERBAUM L.S. Nonlocal Effects in the Core Ionization and Auger Spectra of Small Ammonia Clusters. *The Journal of Physical Chemistry B.* 2011 January 10, **115** pp. 5441–5447

[66] STOYCHEV S. D.,, KULEFF A. I., , CEDERBAUM L. S . Intermolecular Coulombic Decay in Small Biochemically Relevant Hydrogen-Bonded Systems. *Journal of the American Chemical Society.* 2011 April 12, **133** pp. 6817–6824

ICS 71.040.40

Price based on 24 pages